Analysis of Composite Steel-concrete Beams Exposed to Fire using OpenSees

Analysis of Composite Steel-concrete Beams Exposed to Fire Using OpenSees

Jian Jiang[1], Guo-Qiang Li[2] and Asif Usmani[3]

[1] College of Civil Engineering, Tongji University, Shanghai 200092, China. (Corresponding author) Email: jiangjian_0131@163.com

[2] State Key Laboratory for Disaster Reduction in Civil Enginering, Tongji University, Shanghai 200092, China. Email: gqli@tongji.edu.cn

[3]School of Engineering, the University of Edinburgh, Edinburgh EH9 3JF, United Kingdom. Email: asif.usmani@ed.ac.uk

ABSTRACT

OpenSees is an open-source object-oriented software framework developed at UC Berekeley. The OpenSees framework has been recently extended to deal with structural behaviour under fire conditions.This paper summaries the key work done for this extension and focuses on the validation and application of the developed OpenSees to study the behaviour of composite steel-concrete beams under fire conditions. The performance of the developed OpenSees are verified by four mechanical tests and two fire tests on simply supported composite beams. A parametric study is carried out using OpenSees to study the influence of boundary condition as well as composite effect of slab on the behavior of composite beams exposed to fire. The stress and strain along the beam section is output and compared with yield stress limit at elevated temperature to explain these influences in detail. The results show that the stress distribution in the web of the steel beam is more complex due to the support effects.

Keywords: OpenSees; fire condition; composite beam; parametric study; boundary condition.

1. INTRODUCTION

In parallel to research works on the mechanical behavior of composite structures at room temperature, a large number of research works have been carried out throughout the world to better understand the structural responses of composite structures exposed to fire. A composite beam is made with a bare or insulated steel beam and a concrete or a composite

slab connected by shear connectors. The concrete forms the compression flange and the steel provides the tension component. The shear connectors need to have sufficient strength and stiffness to enable the two components to behave as a single structural member. When a composite beam is exposed to fire, thermal gradient developed in the composite beam considering the hot steel beam and relatively cooler slab which produces thermal bowing of the composite beam. The effect of the slab is to restrain the thermal expansion and thermal bowing of the steel beam as well as protect the upper surface of the top flange of the beam from the fire.

The fire performance of composite steel and concrete beams can be assessed by conducting standard fire tests [1-4]. Although the experimental investigation of composite beams in fire gives fundamental understanding of the fire behavior of composite beams, it is very difficult to cover all application domains and robust numerical analysis should be used to make up the experimental limitation [5-19]. Wang et al. [5] developed a computer program for structural analysis at elevated temperature. A comprehensive parametric study was carried out to investigate the influence of beam thermal gradient and axial restraint on the structural responses of composite structures exposed to fire. Wang [6] assessed the effectiveness of a partially protected composite beam by comparing its plastic moment capacity with that of a fully protected beam. A two-dimensional analytical model was proposed by Oven [7] and developed by Dissanayake [8] to consider the partial interaction in composite beams. The shear connectors acted as a continuous shearing medium along the length of the beam and it is difficult to be extended to three-dimensional problems. Huang et al. [9] developed a separate shear connector element permitting modelling of full, partial and zero interaction between the steel beam and concrete slab. Huang et al. [10] presented a three-dimensional nonlinear finite-element procedure for modeling composite steel-framed structures in fire. The model consisted of fibred beam-column, spring and layered slab elements. A two-node spring element of zero length was used to model the semi-rigid beam-column connection. Sanad et al. [11] modeled the Cardington restrained beam test using a grillage of beam elements to investigate the influence of restrained thermal expansion and thermal bowing on the forces and moments developed in the composite structures in fire. Fakury et al [12] presented

two-dimensional finite element analysis of semi-continuous composite beam with different temperature distribution regimes. Benedetti and Mangoni [15] extended the method of the Fourier series expansion to the fire analysis of composite beams concerning deformable shear connectors. Ranzi and Bradford [16] presented an analytical model for structural analysis of composite beams in fire accounting for both longitudinal and transverse interaction by means of the principle of virtual work. However this study is restricted to lower temperatures, temperature dependent elastic material. Lamont et al. [17] studied the structural behavior of a steel-concrete composite frame subjected to a natural fire using ABAQUS. Different protection regimes of internal and external beams were applied and results showed that fire protecting the edge beams provided an increasing level of fire resistance. Hozjan et al. [18] presented a strain-based finite element to account for slip between steel beam and slab. Fang et al. [19] proposed two robustness assessment approaches for steel-framed composite construction under localised fire using a grillage model of beam elements.

These numerical analyses of composite structures at elevated temperature were carried out based on specialist programs such as VULCAN [20, 21], ADAPTIC [22, 23], SAFIR [24], and commercial packages such as ABAQUS [25, 26], ANSYS and DIANA. Although specialist programs are cost-effective to purchase and easy to use they lack generality and versatility. The commercial packages have a large library of finite elements and excellent GUIs to enable efficient and detailed modeling of structural responses to fire. However, commercial packages require substantial recurring investment for purchase and maintenance that often make them unaffordable for researchers.

OpenSees [27] is an open source object-oriented software framework developed at UC Berekeley and supported by PEER and Nees. OpenSees has so far been focussed on providing an advanced finite-element computational tool for analysing the non-linear response of structural frames subjected to seismic excitations. The features of object-oriented programs [28] make OpenSees computationally efficient, flexible, extensible and portable [29-32]. This means a developer can combine and reuse the existing classes in OpenSees to create an application to solve one’s own specific problem.

The static analysis of structures in fire using developed OpenSees has been extensively verified and validated by the authors [33-35]. This paper presents an augmentation of OpenSees to enable a two-dimensional thermomechanical analysis of composite beams. The composite beams are modelled by either a single section or rigid link methods in OpenSees. Four mechanical tests and two fire tests on the composite beams are chosen to verify the performance of the developed OpenSees and the equivalence of the two modeling methods. OpenSees is then used to perform an extensive parametric study in which the effects of boundary conditions on the structural response of a composite beam in fire are considered. This study highlights the importance of the composite effect from the concrete slab and restrained thermal expansion on the fire behavior of the composite beam.

2. OPENSEES MODEL

The theoretical model and class hierarchy developed in the extended OpenSees are presented in details in reference [33] and [34] respectively. Fiber sections are applied for beam/column element in OpenSees and the temperature distribution developed in OpenSees is defined by temperature points located along the height of sections as shown in Figure 1 which shows a general fibre section, which is subdivided into longitudinal fibres. The area, modulus of elasticity and moment of inertia of each fibre *i* are denoted by A_i, E_i, I_i, respectively. The parameter z_i is the distance of the centre of the fibre *i* to the top of the section. Each fibre *i* is subjected to a uniform temperature increment, ΔT_i, and a through-depth thermal gradient, $\left(T_{,z}\right)_i$. The coefficient of thermal expansion is defined as α_i.

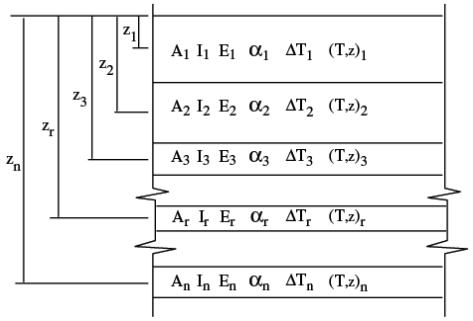

Figure 1: A general section divided into n fibres

The mechanical strain that stress depends on is obtained by subtracting thermal strain from total strain given as

$$\varepsilon_{mechanical} = \varepsilon_{total} - \varepsilon_{thermal} \tag{1}$$

Since the thermal load is defined and applied as well as the material property and mechanical strain are updated at elevated temperature, thermomechanical analysis procedure in OpenSees can then follow the general procedure of mechanical analysis of structures [29, 37]. The flow chart of element state determination of this thermomechanical analysis mentioned above is shown in Reference [33].

The extension of OpenSees involves creating a new thermal load pattern class, and modifying existing material classes to include temperature dependent properties. Figure 2 shows the class hierarchy of new classes added in OpenSees using the graphical Unified Modeling Language notation [38]. New temperature dependent material classes Steel01Thermal (for steel) and Concrete02Thermal (for concrete) were created by modifying the existing material class steel01 and Concrete02 respectively. Steel01 is a bilinear steel material with kinematic hardening and optional isotropic hardening described by a non-linear evolution equation [39]. Concrete02 considers the tensile strength and linear tension softening [40]. The temperature dependence added in these two material classes were based on Eurocode stipulations [41, 42]. The beam element DispBeamColumn2dThermal was created by modifying the existing beam element DispBeamColumn2d [37].

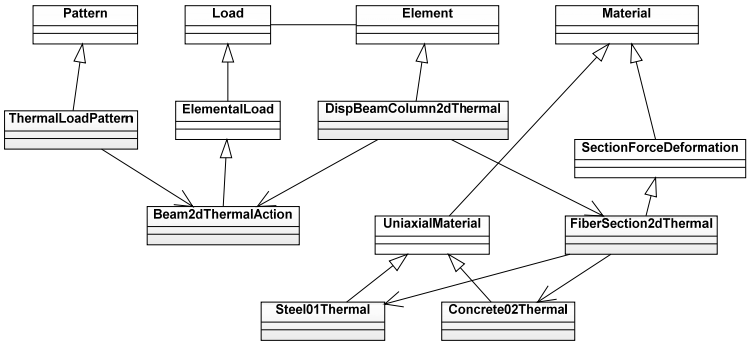

Figure 2: Class diagram for thermomechanical analysis in OpenSees

A composite beam can be modeled in two alternative ways in OpenSees. One is to use a

single section including steel I beam and concrete slab representing the composite beam. The other is to define steel beam and slab separately with rigid link connected between them to model the full shear connection condition. The command “rigidLink” was used to construct a single multi-point constraint [43] between steel beam and slab to model the shear connection relation. Two rigid-link types “bar” and “beam” are offered in OpenSees. The “bar” type only constrains the translational degree-of-freedom and “beam” type constrains both translational and rotational degrees of freedom. In this paper, the “beam” type is used to model the full shear connection between the steel beam and concrete slab. The schematic of these two OpenSees models are shown in Figure 3.

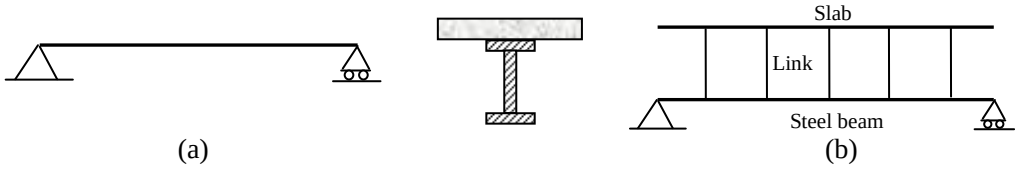

Figure 3: Schematic of OpenSees models for composite beams: (a) single section model; (b) rigid link model.

3. VALIDATION

In this section, the performance of developed structural analysis of composite beams exposed to fire in OpenSees was verified by comparing with experimental results. These comparisons started from four tests on composite beams under mechanical load only followed by two tests on composite beams exposed to standard fire.

3.1 Composite Beams at Ambient Temperature

Four simply-supported composite beams under mechanical load at ambient temperature were analysed using OpenSees. These tests included one tested beam (B4) from Amadio et al. [44] and the other three beams (A3, A5, U4) reported by Chapman and Balakrishnan [45]. The beam U4 was subjected to uniformly distributed load and the others subjected to concentrated load. The test set up and beam dimensions are shown in Figure 4. The existing 2D beam element DispBeamColumn2d was used to model the composite beams in OpenSees. The existing material classes Steel01 and Concrete02 in OpenSees were used to model the steel

and concrete material respectively. The compressive strength of concrete f_c and yield strength of steel beam f_{yb} and reinforcement f_{yr} of tested beams are listed in Table 1. Figure 5 shows the comparisons of mid-span deflection from measured and predicted results of OpenSees as well as Oven [7] and Huang et al. [9]. Good agreement achieved between the single section and rigid link models in OpenSees shows their equivalence to model two-dimensional composite beams under mechanical load. The OpenSees predictions agree well with experiment measurements.

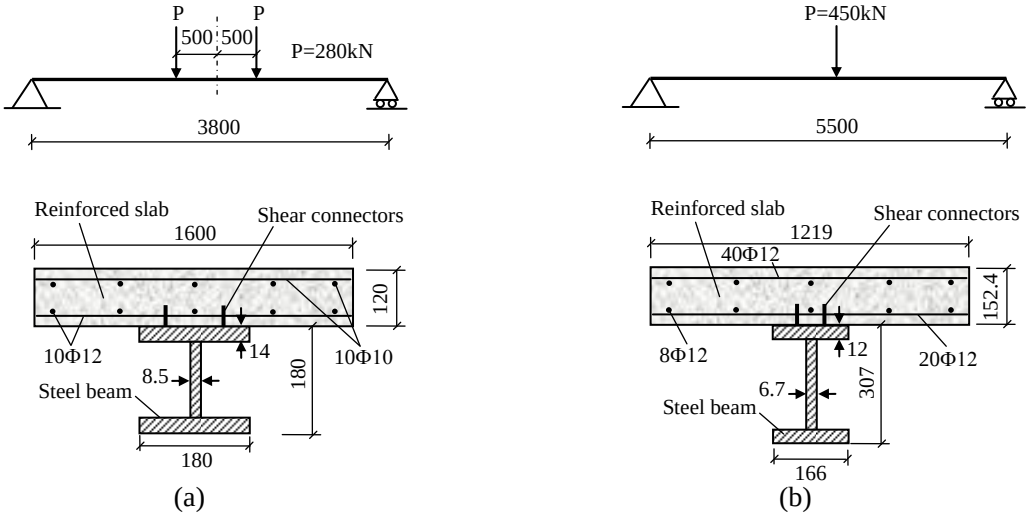

Figure 4: Schematic of tested beams: (a) composite beam B4; (b) composite beam A3, A5 and U4. (all dimensions in mm)

Table 1 Material properties of the tested composite beams

Beam No.	f_{yb} (Mpa)	f_{yr} (Mpa)	f_c (Mpa)
B4 [44]	317	554	41.6
A3 [45]	302	600	27
A5 [45]	290	600	43
U4 [45]	300	600	43
Test 15 and 16 [1]	255	600	30

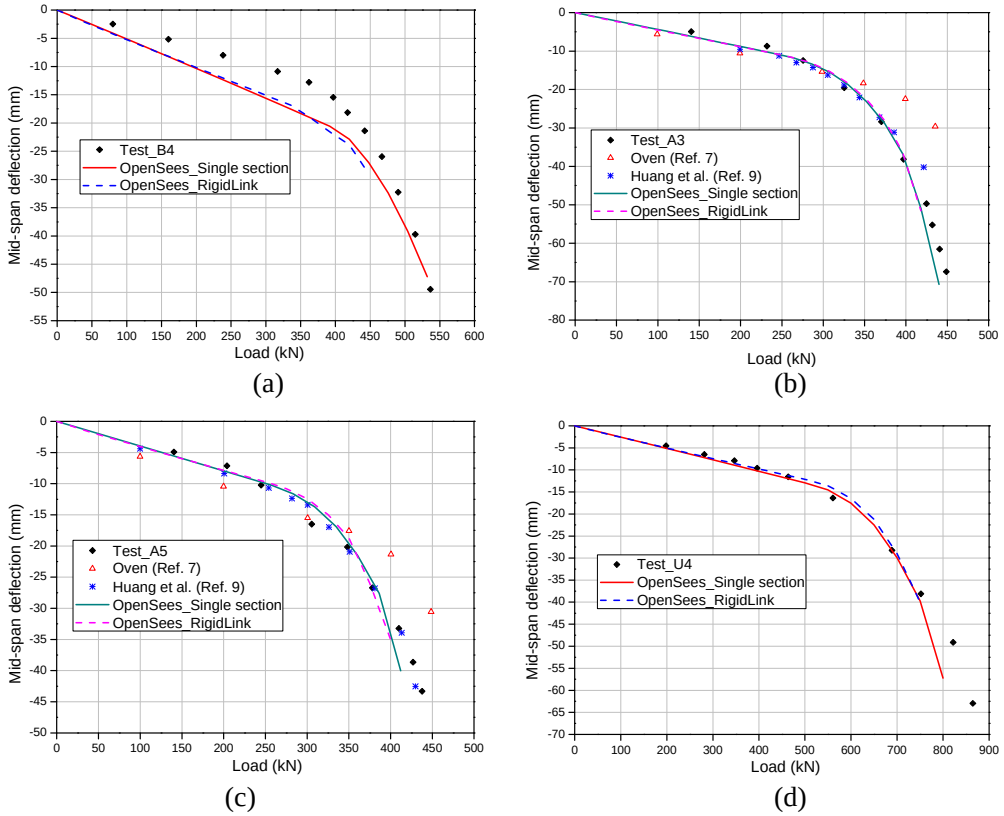

Figure 5: Comparison of measured and predicted mid-span deflection of tested beams: (a) beam B4; (b) beam A3; (c) beam A5; (d) beam U4.

3.2 Composite Beams at Elevated Temperature

Two ISO834 standard fire tests (Test 15 and 16) on simply supported composite beams were conducted by Wainman and Kirby [1]. The structural configuration is shown in Figure 6. The material properties at ambient temperature are shown in Table 1. The material class Steel01Thermal and Concrete02Thermal in OpenSees were used to mode the steel and concrete material in the composite beam. Their temperature dependent properties are shown in Figure 7. The modified beam element DispBeamColumn2dThermal was used to model the composite beams in OpenSees. Figure 8 shows the temperature distribution in different components of the two tested composite beams. No concrete slab temperature profiles were reported and therefore the temperature distributions through the thickness of the slabs were referred to Eurocode 4 [46]. Figure 9 shows the comparisons of mid-span deflection from measured and predicted results of OpenSees and Huang et al. [9]. The OpenSees predictions show reasonable agreement with test results. The equivalence between single section and rigid link models in OpenSees is verified again for composite beams under fire conditions.

Test 15: P=32.47kN; Test 16: P=62.36kN

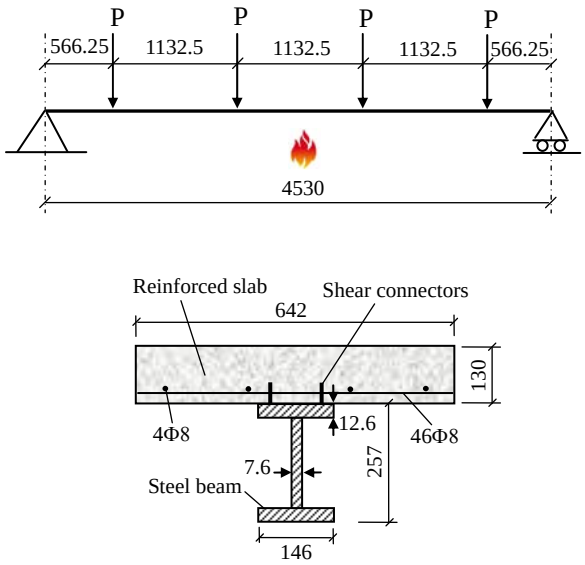

Figure 6: Schematic of tested composite beam (Test 15 and Test 16) (all dimensions in mm)

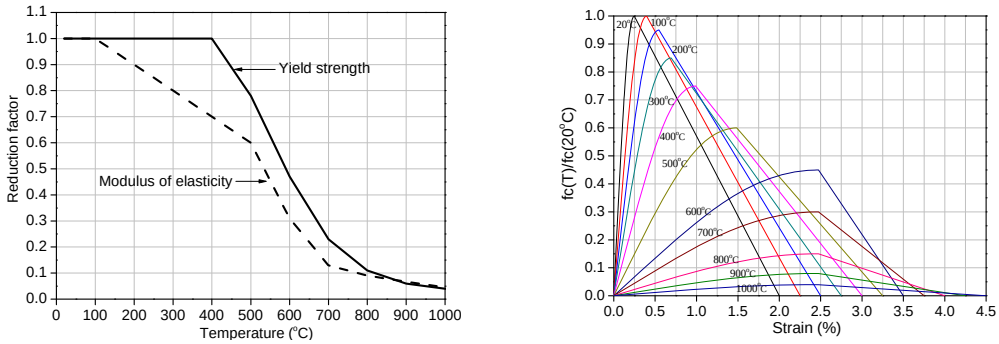

(a) (b)

Figure 7: Material properties at elevated temperature in OpenSees: (a) yield strength and elasticity modulus of steel; (b) compressive stress-strain relation of concrete

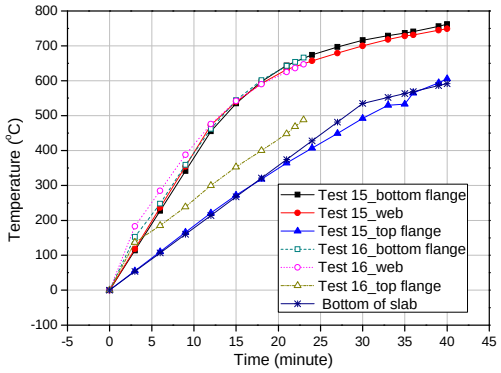

Figure 8: Temperature distribution in the composite beams against time

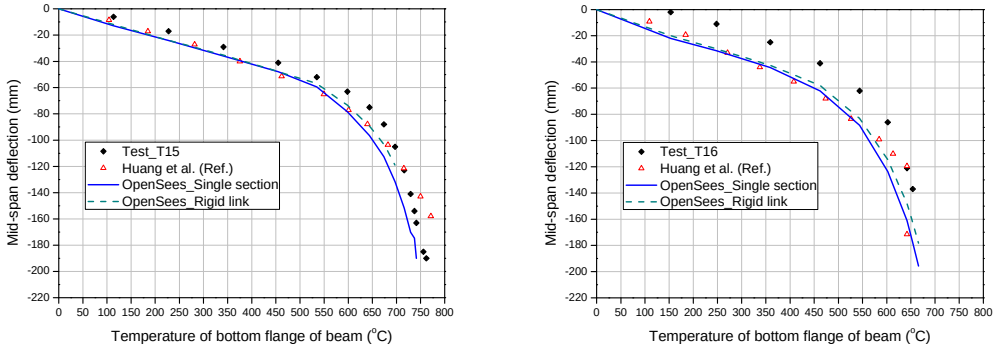

(a) (b)

Figure 9: Comparison of measured and predicted mid-span deflection of tested beams: (a) beam Test 15; (b) beam Test 16.

4. PARAMETRIC STUDY

As the performance of the developed thermomechanical analysis capacity of OpenSees is verified by the above tests on composite beams under mechanical and thermal load, a parametric study on the fire test (Test 15) was carried out in this section to discuss in detail the influence of boundary conditions on the structural responses of composite beams in fire. This analysis is similar to earlier studies by author for the steel beam [33]. In this case, the boundary conditions considered are divided into three categories: simply supported, pinned support (i.e. both ends are translationally restrained but free to rotate) and fully fixed support (i.e. both ends are restrained to translate and rotate). The single section method was used to model the composite beams in OpenSees in this study. The responses of the composite beam for these three support conditions are shown in Figure 10. From Figure 10(a) it can be seen that pinned supported composite beam produces larger mid-span deflection than the simply and fixed supported beam. The horizontal movement of the end of the simply supported beam increases until about 700^{o}C due to the thermal expansion of the composite beam and then begins to decrease due to the increasing deflection of the beam considering material degradation at high temperature. The fixed support causes larger horizontal reaction in the support. Sagging moment exists at mid span of the simply and pinned supported beam but hogging moment for fixed beam.

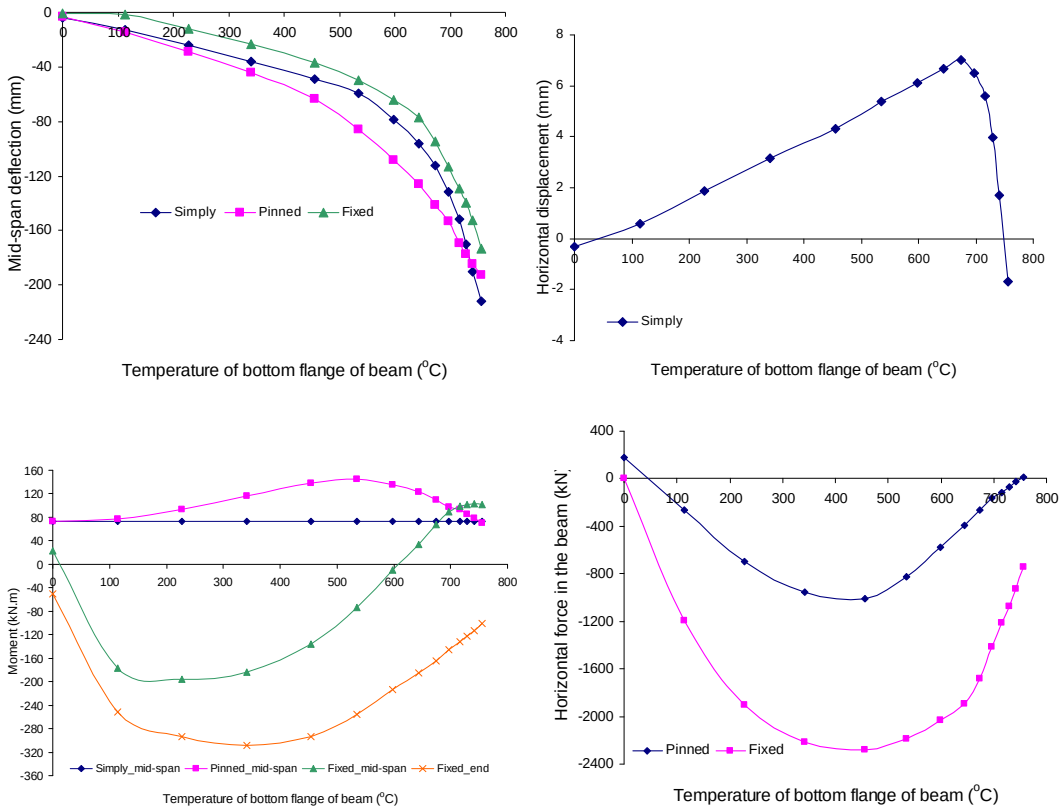

Figure 10: Responses of composite beams exposed to fire with different boundary conditions

Each of these events will be explained in detail with reference to plots of stress and strain distribution along the height of the composite beam section. Then these evens will be further explained by comparing the stress with yield stress and compressive strength of steel and concrete material at elevated temperature.

Figure 11 shows the stress and strain distribution through the section height of the composite beam with three different boundary conditions. The slab stress is magnified 10 times for all cases and the web strain is magnified 2 times only for the simply and pinned beams. Two fibers were defined at the bottom and top flange of the steel beam respectively and four fibers for the web. Total four fibers were defined through the thickness of the concrete slab. The strains through the depth of mid-span beam section for the three boundary conditions show similar pattern and their profiles can be explained as follows. The total strains govern the deformed shape of the structure through kinematic or compatibility considerations. The stress state in the structure depends only on the mechanical strains. For simply supported beam exposed to fire, the mid-span section has a uniform total strain given no rotation in the section.

Considering the composite beam in Test 15 has three sides exposed to fire, it is found that the middle of the web of the section has the highest temperature until 12 minutes and then a bit lower than the bottom flange of the steel beam. If the constant thermal elongation coefficient is assumed, the thermal strain distribution through the depth of the beam section has the similar profile as the temperature distribution. The thermal induced mechanical strain at mid-span section can be obtained by subtracting thermal strain from the uniformly distributed total strain as shown in Figure 12(a). Tensile and compressive strain regions form above and below the centre of the slab respectively. The total mechanical strain can then be derived by combining the thermal induced and external load P induced mechanical load as shown in Figure 12(b). The neutral axis of the composite beam is assumed a bit lower than the center of the slab. There is a small compression region around the middle of the web as well as upper surface of the slab and tension region in the lower components of the steel beam. As temperature continues to increase, bending of the composite beam produces large tensile strain in the whole steel section which gradually cancels and overcomes the compressive strain region in the middle of the web (as shown in Figure 11).

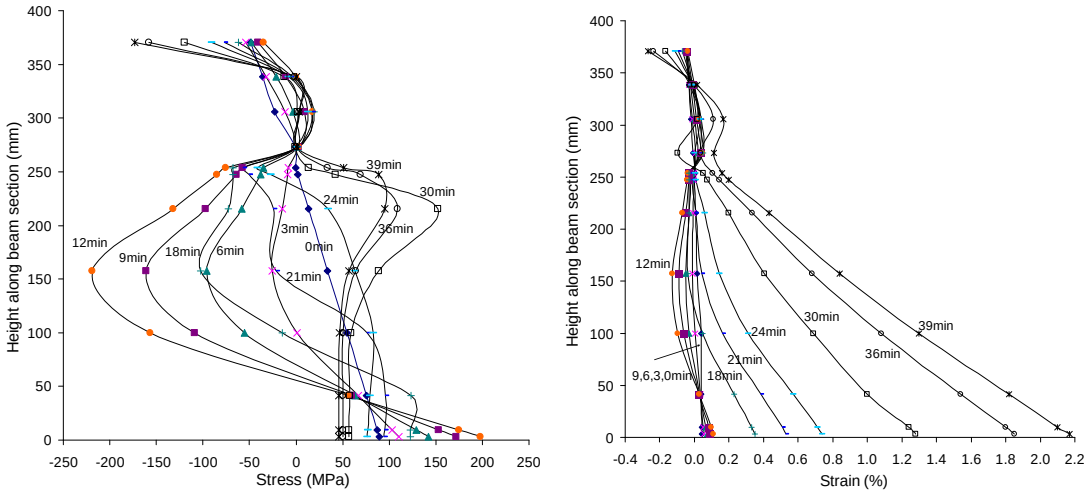

(a)

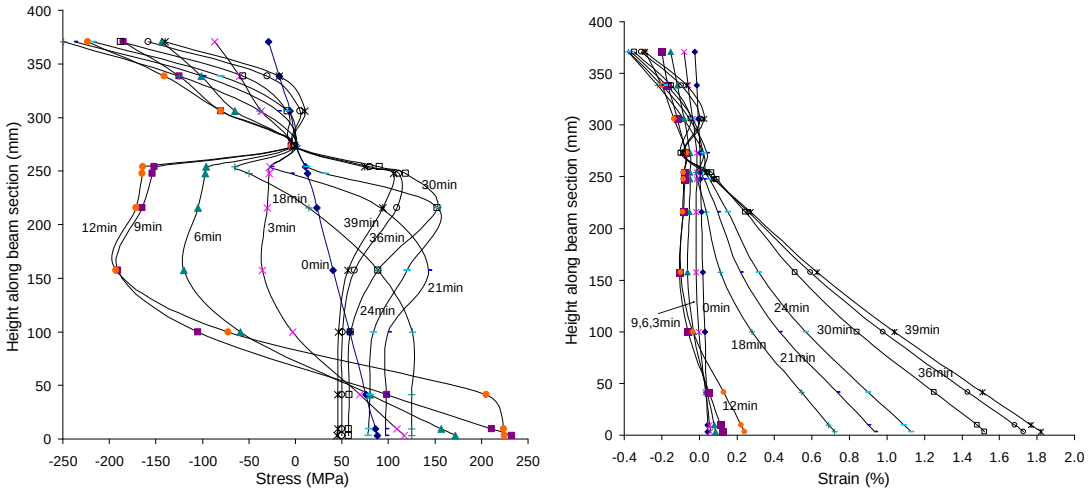

(b)

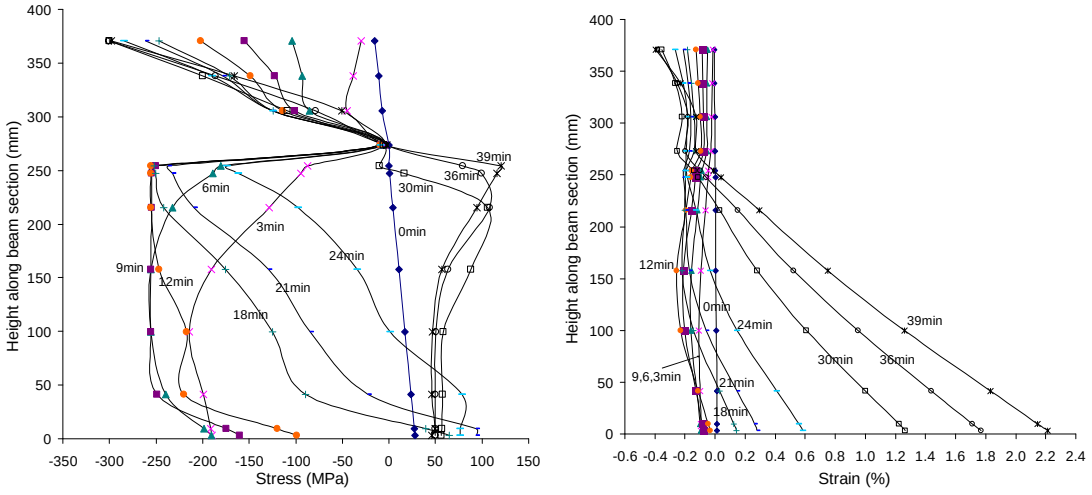

(c)

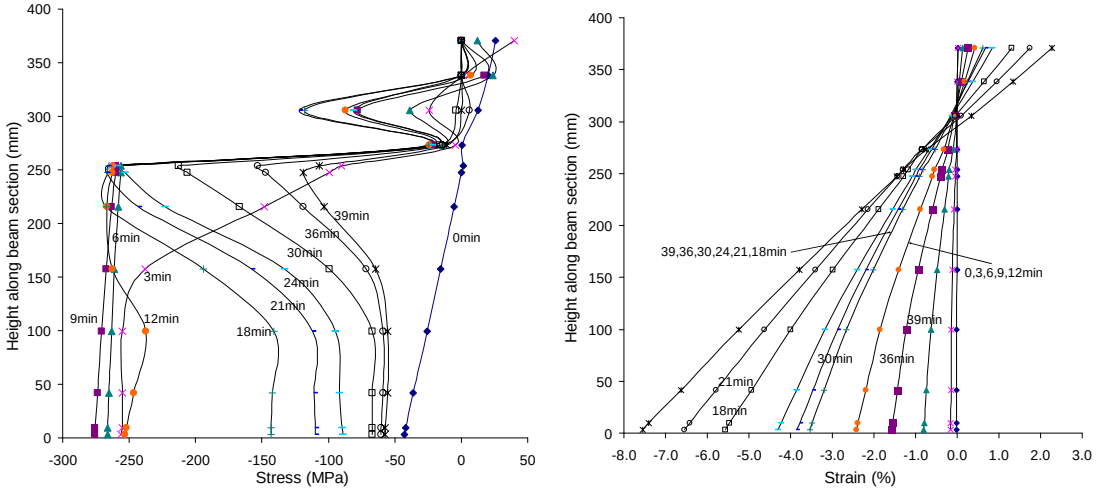

(d)

Figure 11: stress and strain distribution along the height of the beam section against time: (a) mid span of simply supported beam (slab stress×10; slab strain×2) ; (b) mid span of pinned supported beam (slab stress×10; slab strain×2); (c) mid span of fixed beam(slab stress×10); (d) end of fixed beam (slab stress×10).

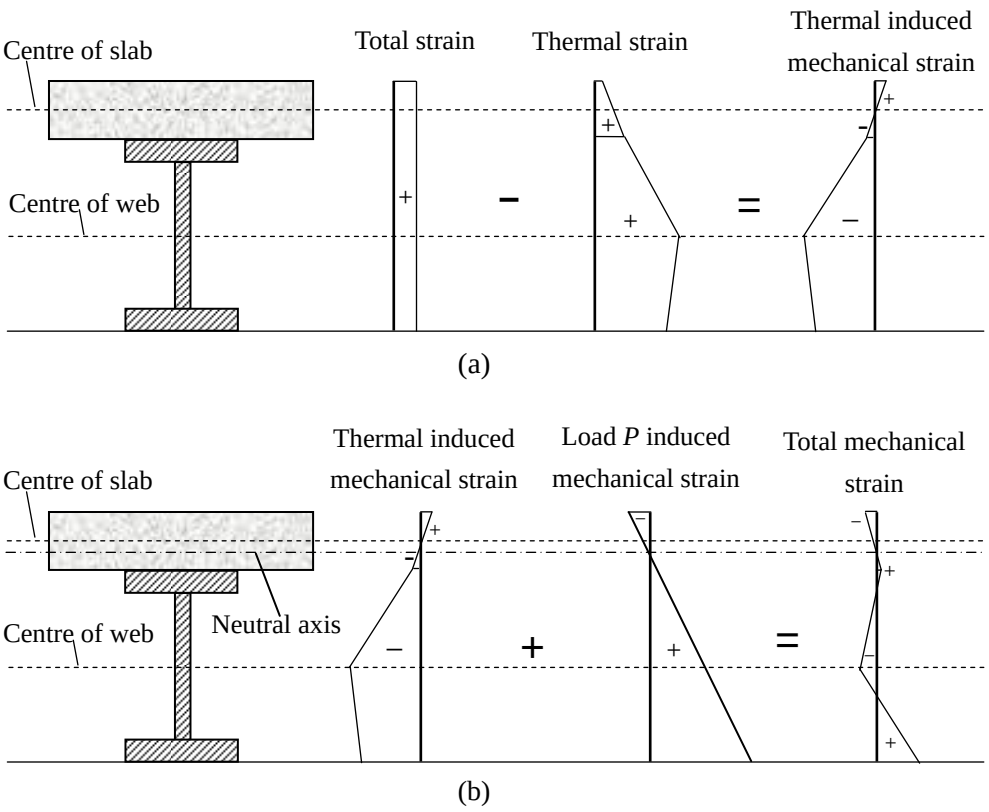

Figure 12: Evolution of strain distributed through the section depth of composite beam: (a) thermal induced mechanical strain; (b) total mechanical strain.

The stress of each fiber can be obtained by multiplying the strain by a temperature dependent Young's modulus. In general the stress at mid span section of the composite beam shows similar pattern that increasing compressive stress exists in the web at early stage of heating and changes to tensile stress at high temperature. The bottom flange of steel beam and top surface of slab is in tension and compression respectively. The largest compressive stress exists in the middle of web and increases as temperature rises as beam heats up until 12 minutes. Then this compressive stress begins to decrease, or tensile stress increases and after 24 minutes the whole section of steel beam is in tension. As the stress in the steel beam changes from compression to tension, the location of largest stress gradually moves from the middle of the web at low temperature to top half of web at high temperature. The differences can be explained in detail as follows by comparing stresses with yield stress limit at elevated temperature in bottom flange, web, top flange and slab components of the composite beam. The yield stress was determined from Figure 7 according to the temperature of different

components as shown in Figure 8.

Bottom flange stress

Figure 13 plots the bottom flange stress of the steel beams with different boundary conditions compared with corresponding yield stress. For simply and pinned supported beams, the thermal gradient in the steel beam leads to downward beam bending, causing increasing tension in the bottom flange at the early stage of heating. After 400 ^{o}C, the tensile stress in the bottom flange begins to decrease due to material degradation and is maintained at reducing tensile yield stress. Compressive stresses build up rapidly within the bottom flange at mid span of the fully fixed beam at early stage of heating. This increase in compressive stress is due to the hogging moment distributed along the beam resulting from the fully fixed support. As temperature continues to increase, this compressive stress is gradually cancelled by increasing tensile stress induced by the beam deflection and finally reversed to tensile stress following the yield stress curve. However the bottom flange stress at the end of the fixed beam increases rapidly form the onset of the fire until the compressive yield stress is reached after 100 ^{o}C. The compressive stress at the end of fixed beam is a bit larger than the yield stress envelope because that strain hardening is considered in material class Steel01Thermal in OpenSees. The large compressive stress in the bottom flange at the end of fixed composite beam will cause local buckling as early as 100 ^{o}C of the fire duration which is also seen in the Cardington tests.

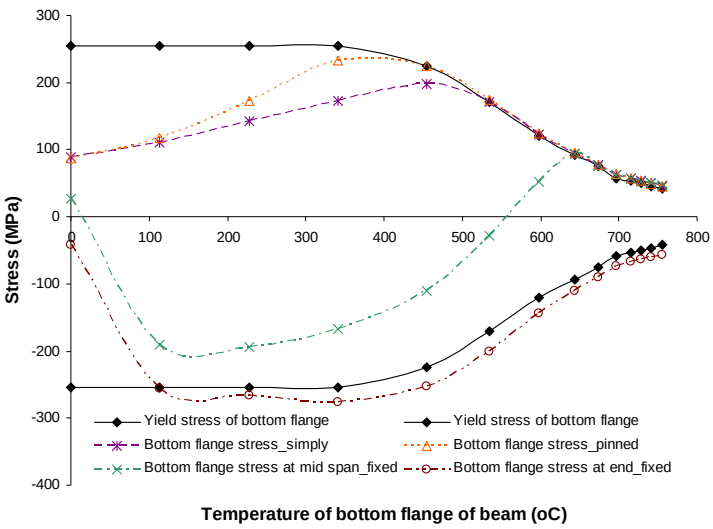

Figure 13: Bottom flange stress of composite beams with different boundary conditions

Web stress

The stress distributions of bottom half, middle and top half web of the composite beam are shown in Figure 14. For simply and pinned supported beam, different from the mid-span bottom flange, the mid-span web stress follows a similar path of increasing compressive stress as the beam heats up and then the compressive stress starts to decrease after 400 ^{o}C. This increasing compressive stress in the web of the steel beam is caused by the restrained thermal expansion of the steel beam by the slab. As temperature increases, the bending of the composite beam produces increasing tension in the whole steel beam considering that the neutral axis lies in the slab. The web stress of fixed beam follows a similar pattern to that of bottom flange. The difference is that the compressive yield stress is reached for the mid-span web stress as early as 200 ^{o}C and remains following the yield stress path.

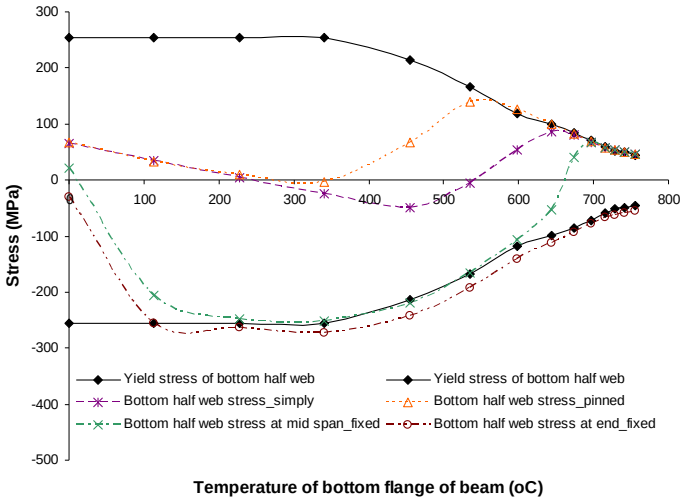

(a)

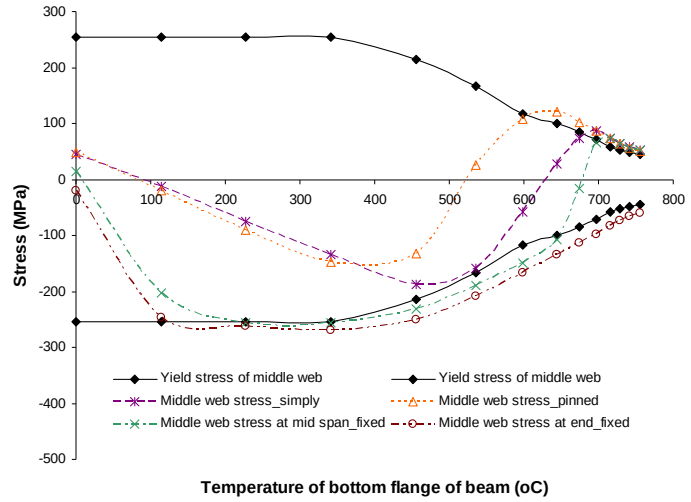

(b)

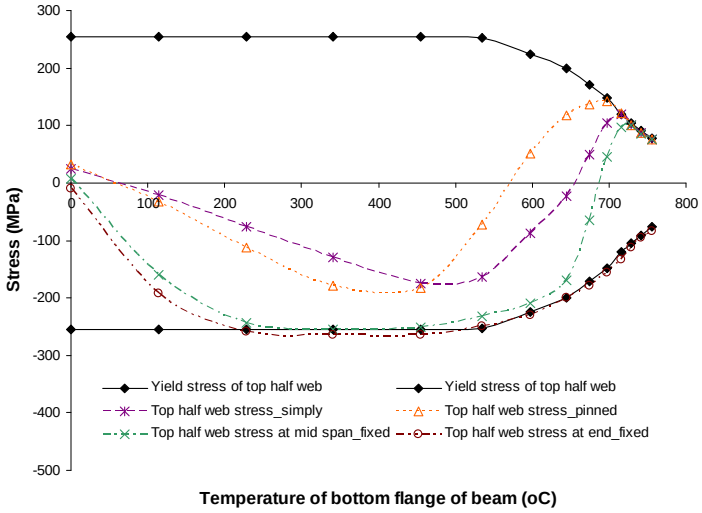

(c)

Figure 14: Web stress of composite beams with different boundary conditions: (a) bottom half of web; (b) middle of web; (c) top half of web

Top flange stress

In general, as shown in Figure 15, the top flange stress is similar to the web stress, with increasing compressive stress at low temperature and increasing tensile stress at high temperature. However the mid-span top flange stress does not reach the yield stress at the whole stage of heating due to lower temperature of the top flange than the web.

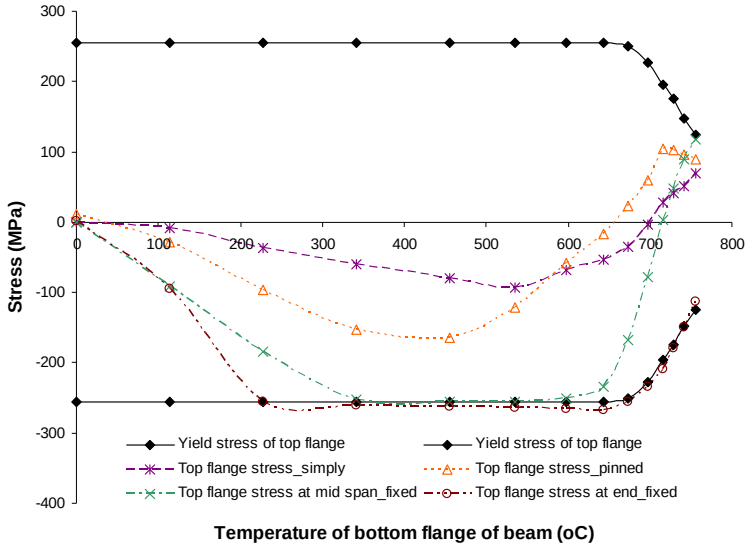

Figure 15: Top flange stress of composite beams with different boundary conditions.

Slab stress

Figure 16 shows the stress variation of top and bottom surface of the slab. The bottom slab stress at mid span of simply supported beam remains in tension before 700 ^{o}C caused by thermal expansion of the steel beam. After 450 ^{o}C the tensile stress begins to decrease which is canceled gradually by the thermal expansion of the slab with significant increasing uniform temperature developed in it. In addition, the bending of the composite beam releases the thermal expansion of the steel beam to some extent which contributes to the decreasing tensile stress. It is interesting to find that after about 700 ^{o}C increasing tensile stress occurs in the bottom of slab. This is because the large deflection of the beam at high temperature produces tension in the bottom of slab considering the neutral axis is near the centre of the slab.

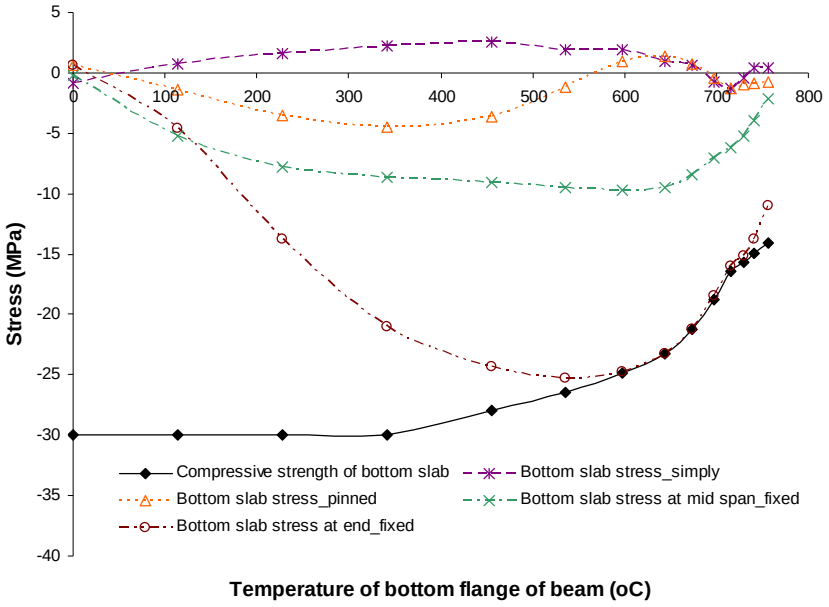

(a)

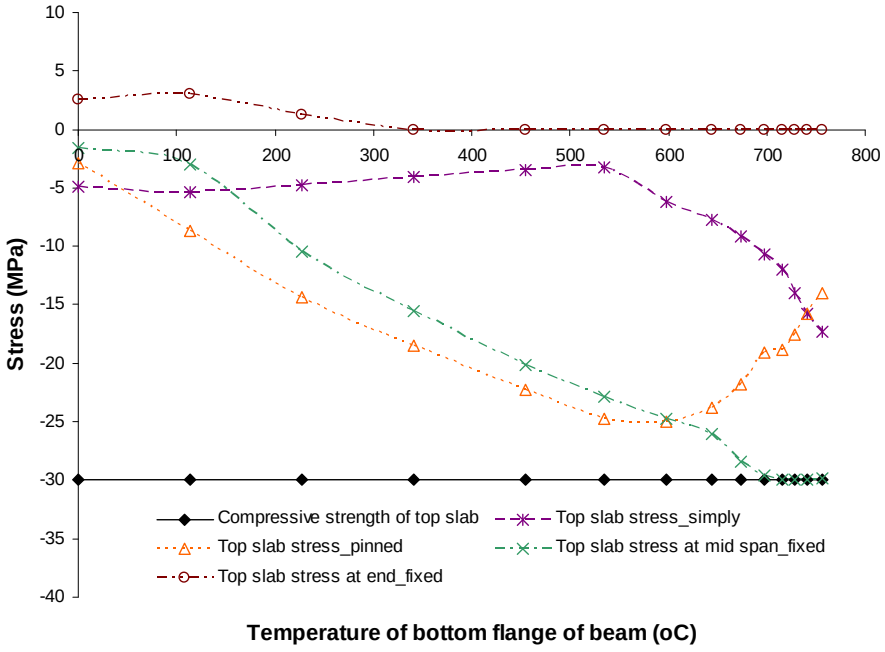

(b)

Figure 16: Slab stress of composite beams with different boundary conditions: (a) bottom of slab; (b) top of slab.

From the aforementioned discussion in the detailed stress distribution in the composite beam it can be seen that compressive and tensile stress exists in different part of the web and slab. It is necessary to further look at the global force in the flange and web of steel beam and slab. Figures 17-20 show the force in the bottom flange, web and top flange of the steel beam as well as total force in the steel beam and slab for different supported beams. For simply

supported beam, as shown in Figure 17, although increasing tension occurs in the bottom flange, the total force in the steel beam shows a similar path of increasing compression at the beginning of heating and increasing tension after about 500 °C as that in web and top flange. This compressive force increase is due to the steel beam's thermal expansion being restrained axially by the relatively cooler concrete slab. As temperature rises, the rapidly increasing deflection relieves much of the axial force. The restrained thermal expansion of the steel beam partly transformed into deflection of the composite beam without causing compression in the steel beam. The compressive force in the slab decreases first and then increases after 500 °C. It is worthy to note that there is a period between 450 °C to 550 °C that the steel beam is in compression and slab in tension.

The force in the steel beam of pinned beam (as shown in Figure 18) shows a similar pattern to that of simply supported beam. However the slab force of pinned supported beam follows a contrary path of increasing compressive force followed by an increasing tensile force after about 450 °C. The resultant force in the pinned composite beam is maintained in compression and changes to tension after 750 °C. As deflection increase and moment capacity decreases with thermal degradation of the beam as shown in Figure 10(c), the beam eventually carries load primarily by catenary action.

For fixed supported beam, all components of the composite beam fall into compression as the beam heats up and begins to decrease with increasing deflection (as shown in Figures 19 and 20). A plateau can be seen in the resultant end force of the fixed beam before the compressive force begins to decrease which is not seen for the simply and pinned beam. After about 400 °C, as the reducing yield stress of steel at elevated temperature, the compressive force in the steel beam begins to decrease and meanwhile significant uniform temperature develops in the concrete slab resulting in a large thermal expansion which produces increasing compressive force in the composite beam. This increasing compressive force due to restrained expansion of slab makes up the decreasing compressive force in the steel beam and maintains the resultant force in the composite beam in a steady condition until this balance is destroyed with increasing material degradation of both steel and concrete. This phenomenon was also observed in Cardington restrained beam test that the horizontal drift at the floor level of the

column connected to the heated beam follows a similar plateau after an initial increase [11]. It is the stabilised horizontal force in the restrained composite beam makes the column stay still. In addition, large tension develops in the top surface of slab at the end of the fixed beam and it will cause concrete cracking which is observed in Cardington tests.

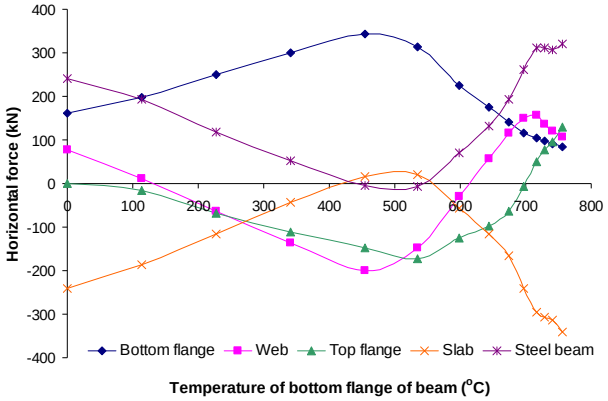

Figure 17: Horizontal force in the simply supported composite beam

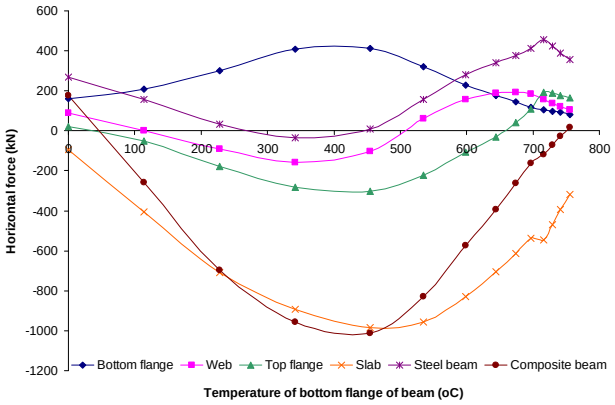

Figure 18: Horizontal force in the pinned supported composite beam

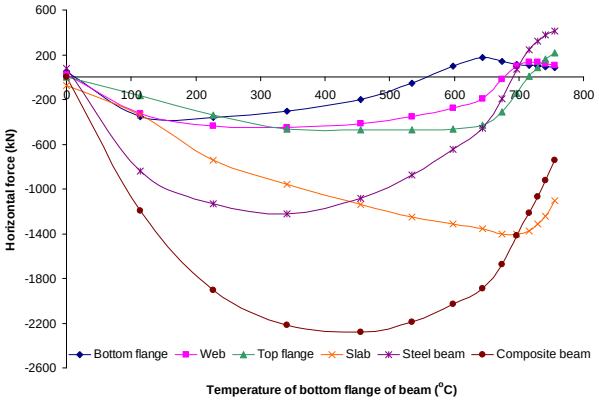

Figure 19:Horizontal force at mid span of fixed supported composite beam

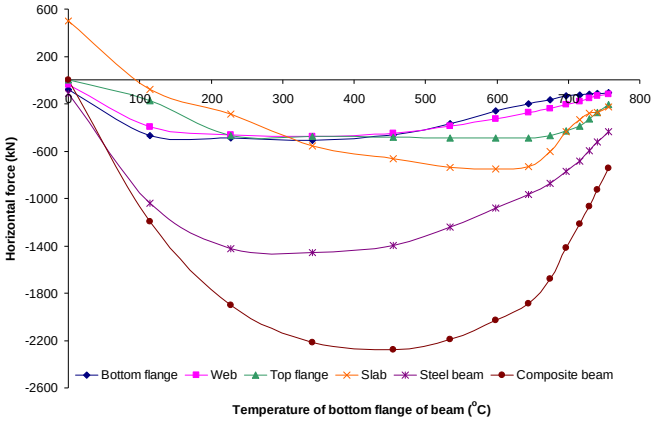

Figure 20: Horizontal force at the end of fixed supported composite beam

5. CONCLUSIONS

The OpenSees framework has been extended to perform thermomechanical analysis of composite structures. The performance of the developed capacity in OpenSees is verified by predicting mid-span deflection of tested composite beam under mechanical and thermal load respectively. Good agreement is achieved between OpenSees predictions and experimental measurements. The single section and rigid link method is proved equivalent to model the composite beam in OpenSees. The further work will focus on modeling three-dimensional steel-framed composite structures using OpenSees (e.g. Cardington tests). The influence of boundary conditions as well as composite effect from concrete slab on the structural responses of composite beams exposed to fire is studied and conclusions can be drawn as follows:

- As deflection increases and moment capacity decreases with material degradation, the pin-pinned supported beam eventually carries load primarily by catenary action which is not the case for simply and fixed supported beam.

- Sagging moment develops at mid span of the simply and pinned supported beam but hogging moment for fixed beam at both mid-span and support. This hogging moment at the end of the fixed beam combined with the restrained thermal expansion produces high tension and compression in the top of slab and bottom flange of the steel beam respectively which makes top slab cracking and bottom flange buckling at very early stage of heating (about 100^{o}C in this case).

- For mid-span local stress distribution, at early stage of heating (before 12 minutes in this case), the middle of the web is in increasing compressive stress and then changed to tensile stress. Meanwhile the location of largest stress gradually moves from the middle of the web at low temperature to top half of web at high temperature. The compression region around the middle of the web is due to the restrained thermal expansion of the steel beam by cooler slab for simply supported beam or support for pinned and fixed beam.

- For simply and pinned supported beam, the tensile bottom flange stress shows convex varying shape of increasing first and decreasing after reaching yield stress. The web and top flange experiences concave stress changes with increasing compressive stress first due to restrained expansion and increasing tensile stress due to beam deflection increase which begins to decrease the yield stress is reached. The whole steel section of fixed beam is in compressive stress and yields at early stage of heating.

REFERENCES

[1] Wainman D.E. and Kirby B.R.. Compendium of UK standard fire test data unprotected structural steel-1. British Steel Corporation, Ref. No. RS/RSC/S10328/1/98/B. Swinden Laboratories, Rotherdam, 1988.

[2] Newman G.M. and Lawson R.M.. Fire resistance of composite beams. The Steel Construction Institute Technical Report 109, 1991

[3] Zhao B. and Kruppa J.. Fire resistance of composite slabs with profiled steel sheet and of composite steel concrete beams, Part 2: Composite beams. CEC, agreement No. 7219/SA/509, CTICM, France, 1995.

[4] Kim M.H., Kim S.D. and Kang S.D.. Behavior of ITECH composite beam in fire-experimental study. Fire Science and Technology, 2007, 26(2): 51-60.

[5] Wang Y.C., Lennon T. and Moore D.B.. The behaviour of steel frames subject to fire. Journal of Constructional Steel Research, 1995, 35: 291-322.

[6] Wang Y.C.. Composite beams with partial fire protection. Fire Safety Journal, 1998, 30:315-332.

[7] Oven V.A. The behaviour of composite beams with partial interaction at elevated temperatures. PhD thesis, The University of Sheffield, UK, 1996.

[8] Dissanayake U.I. The influence of the composite beam-to-steel column joint on the behaviour of composite beams in frames. PhD thesis, The University of Sheffield, UK, 1996.

[9] Huang Z., Burgess I.W. and Plank R.J. Influence of shear connectors on the behaviour of composite steel-framed buildings in fire. Journal of Constructional Steel Research, 1999, 51(3): 219-237.

[10] Huang Z., Burgess I.W. and Plank R.J. Three-dimensional analysis of composite steel-framed buildings in fire. Journal of Structural Engineering, 2000, 126(3): 389-397.

[11] Sanad A.M., Rotter J.M., Usmani A.S. and O'Connor M. Composite beams in large buildings under fire-numerical modeling and structural behaviour. Fire Safety Journal, 2000, 35: 165-188.

[12] Fakury R.H., Las Casas E.B., Pacifico F. and Abreu L.M.P.. Design of semi-continuous composite steel-concrete beams at the fire limit state. Journal of Constructional Steel Research, 2005, 61: 1094-1107.

[13] Wong M.B. and Ghojel J.I.. Strength of steel/conctrete composite beam in fire. Fourth International Conference on Advances in Steel Structures, 2005, 11:973-980.

[14] Zhou H.Y. and Li G.Q. Behavior of steel-composite beams subjected to fire. Fourth International Conference on Advances in Steel Structures, 2005, 11:1005-1010.

[15] Benedetti A. and Mangoni E. Analytical prediction of composite beams response in fire situations. Journal of Constructional Steel Research, 2007, 63: 221-228.

[16] Ranzi G. and Bradford M.A. Composite beams with both longitudinal and transverse partial interaction subjected to elevated temperatures. Engineering Structures, 2007, 29:2737-2750.

[17] Lamont S., Gillie M. and Usmani A.S. Composite steel-framed structures in fire with protected and unprotected edge beams. Journal of Constructional Steel Research, 2007, 63: 1138-1150.

[18] Hozjan T., Saje M., Srpcic S. and Planinc I. Fire analysis of steel-concrete composite beam with interlayer slip. Computers and Structures, 2011, 89: 189-200.

[19] Fang C., Izzuddin B.A., Elghazouli A.Y. and Nethercot D.A. Robustness of steel-composite building structures subject to localised fire. Fire Safety Journal, 2011, 46:348-363.

[20] Huang Z., Burgess I.W. and Plank R.J. Effective stiffness modelling of composite concrete slabs in fire. Engineering Structures, 2000, 22(9): 1133–1144.

[21] Huang Z. The behaviour of reinforced concrete slabs in fire. Fire Safety Journal, 2010, 45: 271-282.

[22] Elghazouli A.Y. and Izzuddin B.A. Response of idealised composite beam-slab systems under fire conditions. Journal of Constructional Steel Research, 2000, 56: 199-224.

[23] Izzuddin B.A., Tao X.Y. and Elghazouli A.Y. Realistic modelling of composite and R/C floor slabs under extreme loading-Part 1: Analytical method. Journal of Structural Engineering, 2004, 130(12): 1972-1984.

[24] Franssen J.M.. SAFIR: a thermal/structural program modelling structures under fire. Proceedings of the North American Steel Construction Conference, April, A.I.S.C. Inc., Baltimore, 2003.

[25] Gillie M., Usmani A.S., and Rotter J.M.. Structural Analysis of the First Cardington Test. Journal of Constructional Steel Research, 2001, 57: 581-601.

[26] Gillie M., Usmani A.S., and Rotter J.M. A Structural Analysis of the Cardington British Steel Corner Test, Journal of Constructional Steel Research, 2002, 58: 427-443.

[27] McKenna, F. T., Object-Oriented Finite Element Programming: Frameworks for Analysis, Algorithms and Parallel Computing, PhD thesis, University of California, Berkeley, 1997.

[28] Booch G.. Object-oriented analysis and design with applications, Addison-Wesley, Reading, Mass, 1994.

[29] McKenna F., Scott M.H. and Fenves G.L. Nonlinear finite-element analysis software architecture using object compositon. Journal of Computing in Civil Engineering, 2010, 24(1): 95-107.

[30] Archer G.C., Fenves G. and Thewalt C. A new object-oriented finite element analysis program architecture. Computers & Structures, 1999, 70: 63-75.

[31] Fenves G.L., McKenna F., Scott M.H. and Takahashi Y. An object-oriented software environment for collaborative network simulation. Proceedings of 13th World Conference on Earthquake Engineering, Canada, 2004

[32] Scott M.H., Fenves G.L., McKenna F. and Filippou F.C. Software patterns for nonlinear beam-column models. Journal of Structural Engineering, 2008, 134(4): 562-571.

[33] Jiang Jian. Nonlinear Thermomechanical Analysis of Structures using OpenSees. PhD Dissertation, University of Edinburgh, Edinburgh, UK, 2012

[34] Jiang J. and Usmani A.S. Modelling of Steel Frame Structures in Fire using OpenSees. Computers & Structures, 2013, 118: 90-99.

[35] Jiang, J., Jiang L.M., Kotsovinos P., Zhang, Jian., Usmani A.S., McKenna, F. and Li G.Q. OpenSees Software Architecture for the Analysis of Structures in Fire. Journal of Computing in Civil Engineering, 2013 (accepted)

[36] Usmani A.S., Rotter J.M., Lamont S., Sanad A.M. and Gillie M.. Fundamental principles of structural behavior under thermal effects. Fire Saftey Journal, 2001, 36(8): 721-744.

[37] Spacone E., Ciampi V. and Filippou F.C. A beam element for seismic damage analysis. Report of University of California, Berkeley, 1992.

[38] Booch G., Rumbaugh J. and Jacobson I. The unified modelling language user's guide, Addison-Wesley, Reading, Mass, 1998.

[39] Mazzoni S., McKenna F., Scott M.H. and Fenves G.L. OpenSees Command Language Manual. University of California, Berkeley, 2007

[40] Yassin M.H.M. Nonlinear analysis of prestressed concrete structures under monotonic and cyclic loads. PhD thesis, University of California, Berkeley, 1994.

[41] Eurocode 2 Design of concrete structures: Part 1.2: General rules, Structural fire design, ENV 1992-1 -2, Brussels, European Committee for Standardisation, 2005.

[42] Eurocode 3 Design of steel structures: Part 1.2: General rules, Structural fire design, ENV 1993-1 -2, Brussels, European Committee for Standardisation, 2005.

[43] Cook, R.D., Malkus, D.S., Plesha, M. E., and Witt, R. J., Concepts and Applications of Finite Element Analysis,4th edition, John Wiley and Sons publishers, 2002.

[44] Amadio C., Fedrigo C., Fragiacomo M. and Macorini L. Experimental evaluation of effective

width in steel-concrete composite beams. Journal of Constructional Steel Research, 2004, 60:199-220.

[45] Chapman J.C. and Balakrishnan S. Experiments on composite beams. The Structural Engineer, 1964, 42(11): 369-383.

[46] Eurocode 4. Design of composite steel and concrete structures: Part 1.2 General rules, Structural fire design, ENV 1994-1 - 2, Brussels, European Committee for Standardisation, 2005